Determination of the Eigenfrequencies of a Ferrite Filled Cylindrical Cavity Resonator using the Finite Element Method

Gilbert C. Chinn, Larry W. Epp, *Member, IEEE*, and Gregory M. Wilkins, *Member, IEEE*

Abstract— **We present a formulation of the Finite Element Method (FEM) particular to axisymmetric problems containing anisotropic media. In particular the resonant frequencies of a longitudinally biased ferrite filled cylindrical cavity are examined. For comparison, a solution of the characteristic equation for the lossless, ferrite filled cylindrical waveguide was modified to give the resonant frequencies of the cylindrical cavity. This analytical solution was then used to examine the error in the FEM formulation for the anisotropic case. It is noted that the FEM formulation for anisotropic material presented, based on both node and edge-based elements, is found to be free of spurious solutions.**

I. Introduction

When analytical solutions are not available the Finite Element Method is commonly used to solve for the eigenfrequencies of inhomogeneously filled electromagnetic cavities and phase constants of inhomogeneously filled waveguides. Formulations using tangential vector elements avoid the problems associated with spurious modes that were common in previous nodal and vectorial based finite element approaches [1-3]. Alternative methods, such as the penalty-method, can also reduce the non-physical modes by explicit enforcement of the divergence free condition. The use of the tangential vector elements has the advantage that no additional penalty term is needed. Also vector elements can be chosen to satisfy tangential continuity at material boundaries as a natural boundary condition. Therefore the use of vector elements often simplifies the analysis.

Thus it is natural to extend tangential vector finite elements to not only inhomogeneities, but to the anisotropic case. Specifically, Wang and Ida [4] were able to show that this extension also can be free of spurious modes. Their method, which was based on the use of tetrahedral and hexahedral elements, was compared to solutions for the inhomogeneous cylindrical cavity. They noted that for permeability tensors without off-diagonal terms, symmetry could be applied to simplify the analysis. A procedure not suitable for ferrite filled cylindrical cavities.

For a ferrite filled cylindrical cavity Dillon *et. al.* [5] applied periodic boundary conditions. This reduces the order of the solution to one-half of the original three dimensional problem, when the appropriate boundary conditions for the modes is applied. A more specific application of the above methods, applied explicitly to axisymmetric cylindrical geometries is detailed here. By applying a Fourier mode expansion to these azimuthally invariant geometries, simplification is inherent. The Fourier modal information is retained, important for the ferrite filled case where the resonant frequencies of the $\pm n$ modes can differ. The FEM analysis is thus effectively reduced to two dimensions.

Axisymmetric geometries of interest in the past included circular waveguides filled with longitudinally biased ferrites. Solutions for the phase constants of these ferrite-filled circular waveguides can be modified for the specific case of the ferrite-filled cavity of interest here. Application of the appropriate boundary conditions then gives a characteristic equation which is solved for the eigenfrequencies. This solution will be outlined here, and used as comparison for the FEM analysis.

II. Finite Element Formulation

The weak form of the vector wave equation for time harmonic electric fields, $\vec{\mathbf{E}} = \vec{\mathbf{E}}(\rho, \phi, z)e^{\jmath\omega t}$, is well known [1]. In the presence of perfectly conducting metallic walls, the weak form becomes:

$$\int_\Omega \left\{ \left(\nabla \times \vec{\mathbf{w}}^t\right) \left(\bar{\mu}_r^{-1} \cdot \left(\nabla \times \vec{\mathbf{E}}\right)\right) - k_0{}^2 \epsilon_r \left(\vec{\mathbf{w}}^t \cdot \vec{\mathbf{E}}\right) \right\} d\Omega = 0 \tag{1}$$

where $k_0{}^2 = \omega^2 \mu_0 \epsilon_0$ and $\vec{\mathbf{w}}^t$ are test functions. Use of Galerkin's method sets the test functions ,$\vec{\mathbf{w}}^t$, equal to $\vec{\mathbf{E}}^*$.

Taking into account the axisymmetry of the problem, the weak form equation is rewritten in electric field components normal and transverse to the ϕ direction. This results in the following bilinear functional:

$$\int_\Omega \left\{ \left(\nabla \times \vec{\mathbf{E}}^*\right) \left(\bar{\mu}_r^{-1} \cdot \left(\nabla \times \vec{\mathbf{E}}\right)\right) - k_0{}^2 \epsilon_r \left[\vec{\mathbf{E}}_t^* \cdot \vec{\mathbf{E}}_t + \mathbf{E}_\phi^* \cdot \mathbf{E}_\phi\right] \right\} d\Omega = 0 \tag{2}$$

where:

$$\nabla \times \vec{\mathbf{E}} = \hat{\mathbf{a}}_\rho \left[\frac{1}{\rho}\hat{\mathbf{a}}_z \cdot \left(\frac{\partial \vec{\mathbf{E}}_t}{\partial \phi}\right) - \hat{\mathbf{a}}_z \cdot \left(\nabla_t \mathbf{E}_\phi\right)\right] + \hat{\mathbf{a}}_\phi \left(\nabla_t \times \vec{\mathbf{E}}_t\right) + \hat{\mathbf{a}}_z \frac{1}{\rho}\left[\mathbf{E}_\phi + \rho\hat{\mathbf{a}}_\rho \cdot \left(\nabla_t \mathbf{E}_\phi\right) - \hat{\mathbf{a}}_\rho \cdot \left(\frac{\partial \vec{\mathbf{E}}_t}{\partial \phi}\right)\right] \tag{3}$$

This work was performed at the Jet Propulsion Laboratory, California Institute of Technology under a contract with the National Aeronautics and Space Administration.

G. C. Chinn and L. W. Epp are with the Jet Propulsion Laboratory, California Institute of Technology, 4800 Oak Grove Drive, Pasadena, CA 91109.
G. M. Wilkins is with the IBM Corporation, Hopewell Junction, NY 12533.

The tensor characterizing a longitudinally biased ferrite is given by:

$$\bar{\mu} = \begin{pmatrix} \mu & -j\mu' & 0 \\ j\mu' & \mu & 0 \\ 0 & 0 & \mu_z \end{pmatrix} \tag{4}$$

The electric field is expanded as a Fourier sum over the harmonics of the azimuthal variable, ϕ, and a sum of finite elements in the ρ-z plane [6]. This allows the eigenvalues, corresponding to the eigenfrequencies here, to be found independently for each value of n. Also, $\mathbf{E}_\phi$ is considered a scalar field over the modelling domain while $\vec{\mathbf{E}}_t$ is a vector field.

$$\mathbf{E}_\phi(\rho,\phi,z) = \sum_n \sum_{i=1}^{N\_nodes} C_\phi(i)\frac{\mathbf{e}_\phi(i)}{\rho}e^{jn\phi}$$
$$\vec{\mathbf{E}}_t(\rho,\phi,z) = \sum_n \sum_{i=1}^{N\_edges} C_t(i)\vec{\mathbf{e}}_t(i)e^{jn\phi} \tag{5}$$

The finite element basis functions, $\mathbf{e}_\phi$, of the $\mathbf{E}_\phi$ field are chosen to be first order triangular nodal elements [7] which are suitable for modelling scalar fields. First order edge-based finite elements [8] are used as the expansion functions, $\vec{\mathbf{e}}_t$, of the $\vec{\mathbf{E}}_t$ field. In order to avoid spurious modes it should be noted that the expansions as given in (5): 1) model the range space and null space of the curl operator sufficiently, and 2) obey tangential continuity boundary conditions between elements [3].

Substitution of the field components expressed in terms of finite elements of (5) in the bilinear functional of (2) along with the inverse of the ferrite tensor given in (3), yields the generalized eigenvalue equation for the cavity:

$$[\mathrm{S}]\{a\} = k_o^2[\mathrm{T}]\{a\} \tag{6}$$

where

$$[\mathrm{S}] = \int_\Omega \left(\nabla\times\vec{\mathbf{E}}^*\right)\left(\bar{\mu}_r^{-1}\cdot\left(\nabla\times\vec{\mathbf{E}}\right)\right)d\Omega \tag{7}$$

and

$$[\mathrm{T}] = \int_\Omega \epsilon_r\left[\vec{\mathbf{E}}_t^*\cdot\vec{\mathbf{E}}_t + \mathbf{E}_\phi^*\cdot\mathbf{E}_\phi\right]d\Omega \tag{8}$$

Here, $\{a\}$ is a vector comprised of the unknown weight coefficients C_ϕ and C_t. We note that our formalism yields sparse real-symmetric [S] and [T] matrices for lossless, Hermitian $\bar{\mu}$ tensors. Consequently, we were able to use standard mathematical library routines to solve the generalized eigenvalue equation.

III. Characteristic Equation

The analytic characteristic equation for cylindrical ferrite structures is due to Kales [9]. In this section, a brief summary of its derivation for the particular case of a metallic cavity is presented. The cavity under consideration has a radius of R and a length of L.

Application of the boundary conditions at the ends of the cavity requires the longitudinal electric field component, $\mathbf{E}_z$, and the transverse magnetic field component, $\vec{\mathbf{H}}_t$, to vary as $\cos(\gamma z)$ while $\mathbf{H}_z$ and $\vec{\mathbf{E}}_t$ must go as $\sin(\gamma z)$ where, $\gamma = (p\pi/L)$. Clearly, there arises two distinct possibilities. First, there are the p = 0 modes which have neither $\mathbf{H}_z$ nor $\mathbf{E}_z$ components. This case will be considered later. Second there exists the p > 0 modes which have both $\mathbf{E}_z$ and $\mathbf{H}_z$ components present. These modes are named HE (EH) if they become TE (TM) modes in the limit when the off diagonal component of the ferrite tensor goes to zero.

The Maxwell equations, for the HE/EH modes, give rise to a pair of coupled wave equations in $\mathbf{E}_z(\rho,\phi)$ and $\mathbf{H}_z(\rho,\phi)$:

$$\begin{aligned} \nabla_t^2\mathbf{H}_z + c\mathbf{H}_z + d\mathbf{E}_z &= 0 \\ \nabla_t^2\mathbf{E}_z + a\mathbf{E}_z + b\mathbf{H}_z &= 0 \end{aligned} \tag{9}$$

where

$$\begin{aligned} a &= \omega^2\epsilon\mu - \omega^2\epsilon\frac{\mu'^2}{\mu} - \gamma^2 \\ b &= -\gamma\omega\frac{\mu_z\mu'}{\mu} \\ c &= \omega^2\epsilon\mu_z - \frac{\mu_z}{\mu}\gamma^2 \\ d &= \gamma\omega\epsilon\frac{\mu'}{\mu} \end{aligned} \tag{10}$$

Again, it is assumed that the fields vary as $e^{j\omega t}$.

This pair can be decoupled by letting:

$$\begin{aligned} \mathbf{E}_z &= \sigma_1 u_1 + \sigma_2 u_2 \\ \mathbf{H}_z &= \frac{\sigma_1 - a}{b}u_1 + \frac{\sigma_2 - a}{b}u_2 \end{aligned}$$

where σ_1 and σ_2 are given by

$$\sigma_{1,2} = \frac{(a+c)\pm\sqrt{(a-c)^2+4bd}}{2} \tag{11}$$

This transformation yields a pair of uncoupled wave equations for the functions u_1 and u_2:

$$\begin{aligned} \nabla_t^2 u_1 + \sigma_1 u_1 &= 0 \\ \nabla_t^2 u_2 + \sigma_2 u_2 &= 0 \end{aligned}$$

The solutions to these equations in cylindrical coordinates gives

$$u_{1,2} = A_{1,2}J_n(\sqrt{\sigma_{1,2}}\rho)e^{jn\phi}$$

where J_n is the Bessel function of order n.

The longitudinal fields are then found by substitution:

$$\mathbf{E}_z = \left(\sigma_1 A_1 J_n(\sqrt{\sigma_1}\rho) + \sigma_2 A_2 J_n(\sqrt{\sigma_2}\rho)\right)e^{jn\phi} \tag{12}$$

$$\mathbf{H}_z = \left(\frac{(\sigma_1 - a)\sigma_1}{b}A_1 J_n(\sqrt{\sigma_1}\rho) + \frac{(\sigma_2 - a)\sigma_2}{b}A_2 J_n(\sqrt{\sigma_2}\rho)\right)e^{jn\phi} \tag{13}$$

The transverse fields can also be expressed in terms of u_1 and u_2 and thus J_n:

$$\vec{\mathbf{E}}_t(\rho,\phi) = \gamma\nabla_t\left[(A_1 J_n(\sqrt{\sigma_1}\rho) + A_2 J_n(\sqrt{\sigma_2}\rho))e^{jn\phi}\right] + \jmath\left(\frac{\mu}{\gamma\mu'}\right)\nabla_t\left[((\sigma_1 - a)A_1 J_n(\sqrt{\sigma_1}\rho) + (\sigma_2 - a)A_2 J_n(\sqrt{\sigma_2}\rho))\,e^{jn\phi}\right] \times \hat{\mathbf{a}}_z \quad (14)$$

$$\vec{\mathbf{H}}_t(\rho,\phi) = \left(\frac{1}{\omega\mu'}\right)\nabla_t\left[((K^2 - \sigma_1)A_1 J_n(\sqrt{\sigma_1}\rho) + (K^2 - \sigma_2)A_2 J_n(\sqrt{\sigma_2}\rho))e^{jn\phi}\right] + \jmath\omega\epsilon\nabla_t\left[(A_1 J_n(\sqrt{\sigma_1}\rho) + A_2 J_n(\sqrt{\sigma_2}\rho))e^{jn\phi}\right] \times \hat{\mathbf{a}}_z \quad (15)$$

where $K^2 = \omega^2\epsilon\mu - \gamma^2$.

The boundary conditions on the side walls of the cavity are now enforced which results in the following pair of equations:

$$\sigma_1 A_1 J_n(\sqrt{\sigma_1}R) + \sigma_2 A_2 J_n(\sqrt{\sigma_2}R) = 0$$

and

$$\frac{\gamma^2 n\mu'}{\mu R}(A_1 J_n(\sqrt{\sigma_1}R) + A_1 J_n(\sqrt{\sigma_1}R)) - (a - \sigma_1)\sqrt{\sigma_1}A_1 J_n'(\sqrt{\sigma_1}R) + (a - \sigma_2)\sqrt{\sigma_2}A_2 J_n'(\sqrt{\sigma_2}R) = 0$$

As usual, the nontrivial solutions are found by setting the determinant of the coefficients of A_1 and A_2 equal to zero. Hence the characteristic equation for the HE/EH modes is

$$\left(\frac{a}{\sigma_2} - 1\right)\sqrt{\sigma_2}\frac{J_n'(\sqrt{\sigma_2}R)}{J_n(\sqrt{\sigma_2}R)} - \left(\frac{a}{\sigma_1} - 1\right)\sqrt{\sigma_1}\frac{J_n'(\sqrt{\sigma_1}R)}{J_n(\sqrt{\sigma_1}R)} + \frac{\gamma^2 n\mu'}{\mu R}\left(\frac{1}{\sigma_1} - \frac{1}{\sigma_2}\right) = 0 \quad (16)$$

where $\sigma_{1,2}$ and a are functions of frequency via equations (10) and (11) and $\gamma = (p\pi/L)$. To determine the HE/EH mode eigenfrequencies, $f_{n,m,p}$, we simply plotted the value of this equation as a function of frequency to determine the zero crossings. Simple bisection was then used to determine the eigenfrequencies to the accuracy desired.

Now consider the p = 0 modes. These modes are identical to the $TM_{n,m,0}$ modes of the empty cavity. Their eigenfrequencies, however, are modified due to the presence of the off-diagonal terms in the ferrite tensor,

$$f_{n,m,0} = \frac{x_{n,m}}{2\pi R\sqrt{\epsilon\mu\left(1 - (\mu'/\mu)^2\right)}} \quad (17)$$

where $x_{n,m}$ is the m-th zero of the n-th order Bessel function.

IV. Numerical Results

A cavity that has a length to radius ratio of 2.0 with a longitudinally biased ferrite tensor permeability given by (4) will be examined. The resonant frequencies have been normalized to the lowest order empty cavity ($\bar{\mu} = \mu_0\mathbf{I}$) resonance: the $TM_{0,1,0}$ mode.

Table 1 shows the first 10 resonances of the cavity and the eigenfrequencies of 2 higher order modes as found by the FEM. The two higher order modes are included for the examination of error related to mesh density in the next section. We generated FEM data on two different meshes, referred to here as Mesh 1 and Mesh 2. Mesh 1 results in 360 unknowns for the n $\neq$ 0 modes and 370 unknowns for the n = 0 modes. The difference is due to the fact that $\mathbf{E}_z$ is completely known on the axis of rotation for the n $\neq$ 0 modes, where it is equal to zero. Similarly, Mesh 2 gives 3686 unknowns for the n $\neq$ 0 modes and 3752 unknowns for the n = 0 modes. The two meshes used the following relative permeability/permittivity values: $\mu = 1.0$, $\mu_z = 1.0$, $\mu' = 0.1$ and $\epsilon = 1.0$.

TABLE 1
Comparison of Cavity Resonances between Characteristic Equation and FEM data from two different meshes

mode	f_{res}/f_0 Char. EQ	f_{res}/f_0 FEM Mesh 1	% error	f_{res}/f_0 FEM Mesh 2	% error
$HE^+_{1,1,1}$	0.9900	0.9987	0.88	0.9909	0.09
$TM_{0,1,0}$	1.0050	1.0040	0.10	1.0050	0.00
$HE^-_{1,1,1}$	1.0257	1.0342	0.83	1.0266	0.09
$EH_{0,1,1}$	1.1991	1.2092	0.84	1.2002	0.09
$HE^+_{2,1,1}$	1.4177	1.4261	0.59	1.4187	0.07
$HE^-_{2,1,1}$	1.4403	1.4492	0.62	1.4414	0.08
$HE^+_{1,1,2}$	1.4697	1.4943	1.67	1.4719	0.15
$HE^-_{1,1,2}$	1.5643	1.5853	1.34	1.5664	0.13
$TM^+_{1,1,0}$	1.6014	1.6119	0.66	1.6033	0.12
$TM^-_{1,1,0}$	1.6014	1.6134	0.75	1.6033	0.12
	⋮	⋮		⋮	
$EH_{0,1,4}$	2.7682	2.8303	2.24	2.7733	0.18
$HE_{0,3,1}$	2.9903	3.0666	2.55	3.0182	0.93
	⋮	⋮		⋮	

Table 1 shows the FEM solution agrees to within 1% of those predicted by the analytical solution for Mesh 2. Moreover, no spurious solutions were present in the solution set. We note that modes with higher values of p or m suffer more error. These modes have higher field variation in the z and ρ directions, respectively.

Figure 1 exhibits the resonant frequencies of the first six modes as a function of the magnitude of the ratio $|\mu'/\mu|$. The magnitude of this ratio is, of course, proportional to the dc biasing field on the ferrite. The solid line curves come from the characteristic equation. The relative permeability/permittivity values used were: $\epsilon = 1.0$, $\mu = 1.0$ and $\mu_z = 1.0$.

V. FEM Error as a Function of Mesh Density

In this section we look at the error as a function of mesh density for two particular resonant frequencies of the ferrite filled cylindrical cavity: the $EH_{0,1,4}$ mode and the $HE_{0,3,1}$ mode. These modes are chosen because they have more field variation in one direction, with a simple first index variation in the other direction. The effects of varying the sampling density in one direction, while keeping the density constant in the orthogonal direction, is to be determined.

The $HE_{0,3,1}$ mode has 5 half-wavelength variations in the ρ direction and a single half-wavelength variation in the z direction. Figure 2 considers the error as a function of the sampling density in the ρ direction. The two curves correspond to the cases where the sampling is 40 and 48 nodes per wavelength in the z direction. Figure 2 shows that both these densities allow similar resolution of the z component of the fields. Assuming that the field is properly modelled in the z direction, Fig. 2 shows that a sampling density of approximately 5 times per wavelength in ρ achieves 1.0% accuracy.

The $EH_{0,1,4}$ mode has 4 half-wavelengths of field variation in the z direction but only one in the ρ direction. The two curves in Figure 3 correspond to the cases where we have sampled 5 and 10 times per wavelength in the ρ direction. Here again increasing the sampling density in the direction of higher field variation leads to more accurate results. Although, Fig. 3 more clearly shows the effect of the sampling density in the orthogonal direction. Thus increasing the sampling density from 5 nodes per wavelength variation to 10 in the ρ direction significantly decreases the error.

VI. Conclusions

We have determined the eigenfrequencies of a ferrite filled cylindrical resonator using the FEM. An FEM formulation which exploits the inherent axisymmetry of the problem has been developed. This method expands the electric field using both node and edge-based elements on a two-dimensional mesh. The resulting solutions are compared to the analytical eigenvalues and found to be free of spurious modes. A brief discussion of the accuracy and the error in this formulation has been provided.

Acknowledgement

The authors thank Daniel J. Hoppe of the Jet Propulsion Laboratory for his illuminating insights and many useful discussions. Support for this computing research was provided by the JPL Supercomputing Project on the CRAY computers at the Jet Propulsion Laboratory and at Goddard Space Flight Center. The JPL Supercomputing Project is sponsored by the Jet Propulsion Laboratory and the NASA Office of Space Sciences and Applications.

References

[1] J. S. Wang and N. Ida, "Eigenvalue analysis in electromagnetic cavities using divergence free finite elements," *IEEE Trans. Magnetics*, vol. 27, no. 5, pp. 3978-3981, Sept. 1991.

[2] J. F. Lee, D. K. Sun and Z. J. Cendes, "Full-wave analysis of dielectric waveguides using tangential vector finite elements," *IEEE Trans. MTT*, vol. 39, no. 8, pp. 1262-1271, Aug. 1991.

[3] Z. J. Cendes, "Vector finite elements for electromagnetic field computation," *IEEE Trans. Magnetics*, vol. 27, no. 5, pp. 3958-3966, Sept. 1991.

[4] J. S. Wang and N. Ida, "Eigenvalue analysis in anisotropically loaded electromagnetic cavities using "edge" finite elements," *IEEE Trans. Magnetics*, vol. 28, no. 2, pp. 1438-1441, March 1992.

[5] B. M. Dillon, A. A. P. Gibson, and J. P. Webb, "Cut-off and phase constants of partially filled axially magnetized, gyromagnetic waveguides using finite elements," *IEEE Trans. on Microwave Theory and Tech.*, vol. 41, no. 5, pp. 1438-1441, May 1993.

[6] D. J. Hoppe, L. W. Epp and J. F. Lee, "A hybrid symmetric FEM/MOM formulation applied to scattering by inhomogeneous bodies of revolution," *submitted for publication in IEEE Trans. Antennas Propagat.*

[7] P. Silvester and R. Ferrari, *Finite Elements for Electrical Engineers*. Cambridge, England: Cambridge Univ. Press, 1990.

[8] A. Bossavit and I. Mayergoyz, "Edge-elements for scattering problems," *IEEE Trans. Magnetics*, vol. 25, no. 4, pp. 2816-2821, July 1989.

[9] M. L. Kales, "Modes in wave guides containing ferrites," *J. Applied Physics*, vol. 24, no. 5, pp. 604-608, May 1953.

Gilbert C. Chinn received a B.S.E.E. degree from UCLA in 1988 and a M.S.E.E. degree from UCSB in 1990. He is currently pursuing a M.S. in Physics at CSULA and is a Member of the Technical Staff at the Jet Propulsion Laboratory in Pasadena, CA. His interests include numerical electromagnetics and mathematical physics.

Larry W. Epp received the B.S.E.E. degree from Bradley University, Peoria, IL in 1984. After working briefly for TRW in Redondo Beach, CA he returned to Illinois where he received the M.S. and Ph.D. degrees in electrical engineering from the University of Illinois in 1986 and 1990 respectively. Upon completion of a Post Doctorate with Prof. Raj Mittra at the Electromagnetic Communication Laboratory, University of Illinois, he has been with the Jet Propulsion Laboratory in Pasadena, CA working on dichroic plates for the NASA/JPL Deep Space Network. His research interests include frequency selective surfaces, finite and lossy periodic structures, active surfaces, and numerical techniques.

Gregory M. Wilkins was born in Washington, DC, on March 3, 1960. He received the degree of bachelor of science in electrical engineering from the University of Maryland, College Park, in 1983 and the master of science degree in electrical engineering from the Johns Hopkins University in 1984. In 1992 he completed his Ph.D. degree in electrical engineering at the University of Illinois. Since then he has been with the IBM Corporation in Hopewell Junction, NY. His current research interests include electromagnetic modelling of high-speed digital circuits and electronic packaging.

Figure Titles

Fig. 1. Normalized resonant frequencies of the first six modes of the ferrite filled cylindrical cavity as a function of the ratio of $|\mu'/\mu|$.

Fig. 2. Error as a function of the sampling density in the ρ direction.

Fig. 3. Error as a function of the sampling density in the z direction.

Fig. 1. Normalized resonant frequencies of the first six modes of the ferrite filled cylindrical cavity as a function of the ratio of $|\mu' / \mu|$

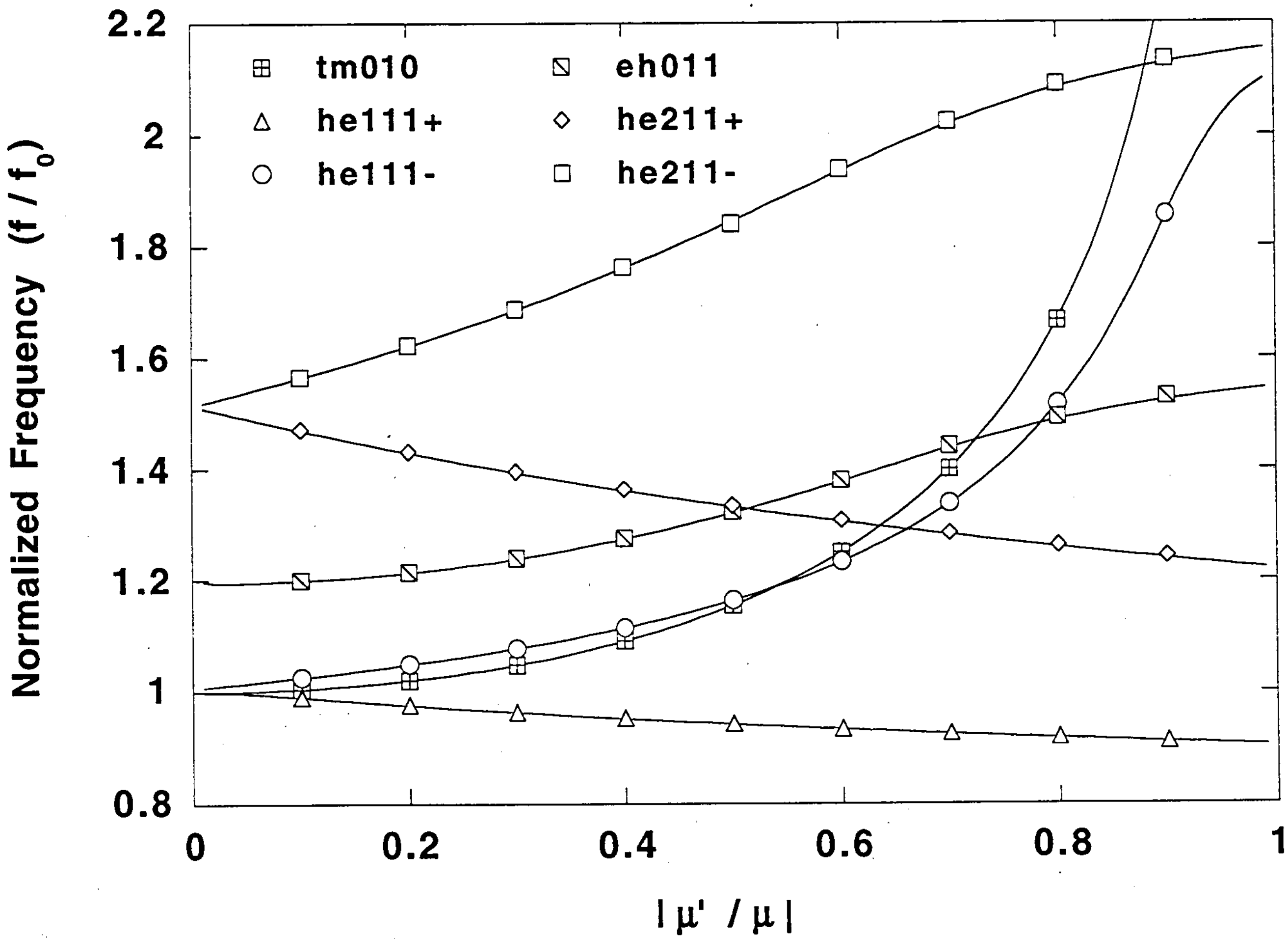

Fig. 2. Error as a function of the sampling density in the ρ direction

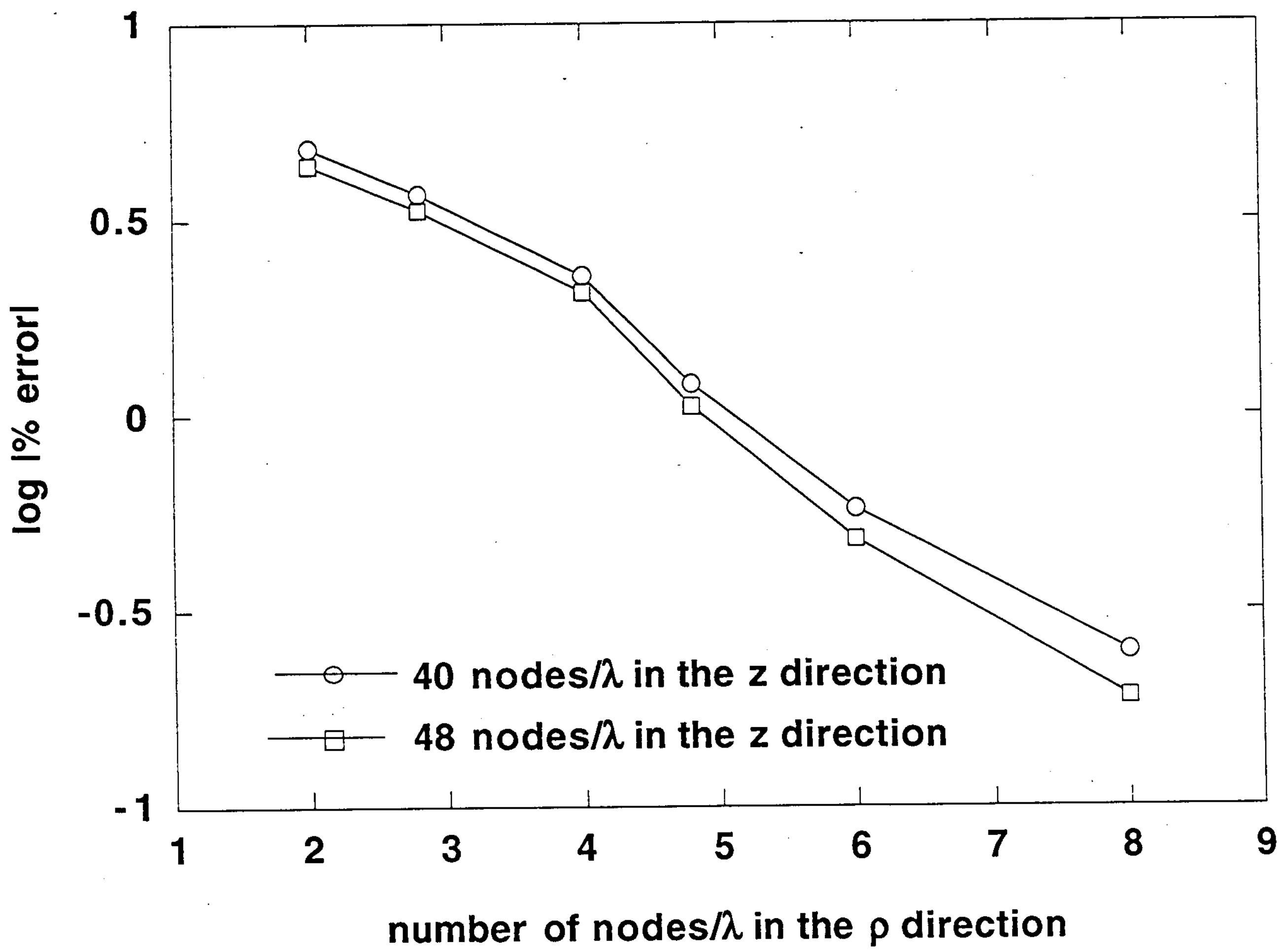

Fig. 3. Error as a function of the sampling density in the z direction